Since January 2020 Elsevier has created a COVID-19 resource centre with free information in English and Mandarin on the novel coronavirus COVID-19. The COVID-19 resource centre is hosted on Elsevier Connect, the company's public news and information website.

Veterinary Microbiology 221 (2018) 49–58

Contents lists available at ScienceDirect

Veterinary Microbiology

journal homepage: www.elsevier.com/locate/vetmic

Susceptibility of porcine IPEC-J2 intestinal epithelial cells to infection with porcine deltacoronavirus (PDCoV) and serum cytokine responses of gnotobiotic pigs to acute infection with IPEC-J2 cell culture-passaged PDCoV

Kwonil Jung[a,*], Ayako Miyazaki[a,b], Hui Hu[a,c], Linda J. Saif[a,*]

[a] Food Animal Health Research Program, Ohio Agricultural Research and Development Center, College of Food, Agricultural and Environmental Sciences, Department of Veterinary Preventive Medicine, The Ohio State University, Wooster, OH, USA
[b] Division of Virology and Epidemiology, National Institute of Animal Health, National Agriculture and Food Research Organization, Tsukuba, Ibaraki, Japan
[c] College of Animal Science and Veterinary Medicine, Henan Agricultural University, Zhengzhou, China

ARTICLE INFO

Keywords:
IPEC-J2
Porcine deltacoronavirus
Cell death
Virus
Pig

ABSTRACT

The porcine small intestinal epithelial cell line, IPEC-J2, is useful to characterize the interactions of enterocytes with enteric viruses *in vitro*. We investigated whether IPEC-J2 cells are susceptible to porcine deltacoronavirus (PDCoV) infection. We conducted quantification of infectious virus or viral RNA, immunofluorescent (IF) staining for the detection of PDCoV antigens, and TUNEL assay in IPEC-J2 cells inoculated with the strain OH-FD22-P8 grown in LLC-PK cells, and supplemented with 10 μg/ml of trypsin in the cell culture medium. Cytopathic effects (CPE) that consisted of enlarged and rounded cells followed by cell shrinkage and detachment, were identified by the 3rd viral passage in the IPEC-J2 cells. PDCoV antigen was detected in the cells showing CPE. By double IF and TUNEL staining, most PDCoV antigen-positive IPEC-J2 cells failed to show TUNEL-positive signals, indicating that PDCoV-infected IPEC-J2 cells may not undergo apoptosis, but rather necrosis, similar to necrotic cell death of infected enterocytes *in vivo*. There was increased interleukin-6 in PDCoV-infected IPEC-J2 cell culture supernatants at post-inoculation hour (PIH) 48–96, as evaluated by ELISA, concurrent with increased titers of PDCoV at PIH 24–72. The susceptibility of IPEC-J2 cells to PDCoV infection supports their usefulness to characterize the interactions of enterocytes with PDCoV. We also demonstrated that IPEC-J2 cell culture-passaged PDCoV (OH-FD22-P8-I-P4) was enteropathogenic in 10-day-old gnotobiotic pigs, and induced systemic innate and pro-inflammatory cytokine responses during the acute PDCoV infection.

1. Introduction

Porcine deltacoronavirus (PDCoV), a member of the genus *Deltacoronavirus* in the family *Coronaviridae* of the order *Nidovirales*, causes acute diarrhea, vomiting, dehydration and mortality in nursing pigs (Jung et al., 2015b; Lau et al., 2012). PDCoV has been successfully isolated and propagated in two epithelial cell lines of swine origin, LLC porcine kidney (LLC-PK) and swine testicular (ST) cells (Hu et al., 2015). The optimal cell culture conditions to isolate and propagate PDCoV in LLC-PK and ST cells required supplementation of 10 μg/ml of trypsin and 1% pancreatin in the cell culture maintenance medium, respectively (Hu et al., 2015). The addition of trypsin and pancreatin in the PDCoV-inoculated LLC-PK and ST cells, respectively, resulted in similar cytopathic effects (CPE) that consisted of enlarged, rounded, and densely granular cells that occurred singly or in clusters, followed by cell shrinkage and detachment as a result of apoptotic cell death (Jung et al., 2016). On the other hand, infected enterocytes *in vivo* appeared to acutely undergo vacuolar degeneration and exfoliated extensively from the villous epithelium, followed by villous atrophy (Chen et al., 2015; Jung et al., 2015b). This process might be associated with necrosis of the infected enterocytes (Jung et al., 2016).

The porcine enterocyte cell line, IPEC-J2, is a non-transformed, stable small intestinal columnar epithelial cell line (Brosnahan and Brown, 2012; Vergauwen, 2015). The cells were originally isolated from the mid-jejunal epithelium of a neonatal unsuckled piglet in 1989 at the University of North Carolina (Brosnahan and Brown, 2012; Vergauwen, 2015). Because of the significant physiologic and morphologic similarities to enterocytes *in vivo*, this primary cell line has been used increasingly to characterize the interactions of intestinal epithelial cells with enteric bacteria and viruses *in vitro*. IPEC-J2 cells

* Corresponding authors.
E-mail addresses: jung.221@osu.edu (K. Jung), saif.2@osu.edu (L.J. Saif).

https://doi.org/10.1016/j.vetmic.2018.05.019
Received 10 April 2018; Received in revised form 24 May 2018; Accepted 29 May 2018

have been infected with porcine epidemic diarrhea virus (PEDV) and transmissible gastroenteritis virus (TGEV) (Lin et al., 2017; Shi et al., 2017; Xia et al., 2017; Zhao et al., 2014). Compared with PEDV-infected Vero (African green monkey kidney) cells (Guo et al., 2016), the proteomic data from PEDV-infected IPEC-J2 cells appeared to better coincide with the physiologic and pathologic outcomes in PEDV-infected enterocytes *in vivo* (Lin et al., 2017).

In our previous study, IPEC-J2 cells were also evaluated in parallel with LLC-PK and ST cells (Hu et al., 2015). However, IPEC-J2 cells failed to efficiently support the isolation and propagation of PDCoV, despite the fact that IPEC-J2 cells originate from villous enterocytes in the small intestine that are the main site of PDCoV infection *in vivo*. We hypothesized that the lower susceptibility of IPEC-J2 cells to initial infection with PDCoV, compared with LLC-PK or ST cells, could have been increased if virus of higher titer, than that contained in the original fecal samples (Hu et al., 2015), was used as inoculum in IPEC-J2 cells. Therefore, we used the cell culture-adapted PDCoV to investigate: i) whether porcine IPEC-J2 cells are susceptible to infection with cell culture-adapted PDCoV; ii) the cell death mechanism, necrosis or apoptosis, by which PDCoV causes death of infected IPEC-J2 cells *in vitro*; iii) if the cell death of PDCoV-infected IPEC-J2 cells *in vitro* resembles necrosis of infected enterocytes *in vivo*; and iv) whether PDCoV infection induces altered or increased pro-inflammatory or innate cytokine responses in supernatants of IPEC-J2 cells *in vitro* and in the serum of infected gnotobiotic (Gn) pigs *in vivo*. For the *in vivo* study, we inoculated Gn piglets with the IPEC-J2 cell culture-passaged PDCoV to examine the enteropathogenicity and the induction of innate and pro-inflammatory cytokines in the sera during the acute PDCoV infection.

2. Materials and methods

2.1. Virus

The PDCoV OH-FD22-P8 (passage 8) virus was serially passaged in LLC-PK (ATCC CL-101) cells supplemented with trypsin (10 μg/ml) in the cell culture medium for a total of 8 passages, as described previously (Hu et al., 2015). After the 6th passage, the virus was purified once by a plaque assay and then further serially passaged (Hu et al., 2015). The viral RNA titer of the OH-FD22-P8 used in this study was 10.5 $\log_{10}$ genomic equivalents (GE)/ml, and the infectious titer was 8.6 $\log_{10}$ plaque forming units (PFU)/ml.

2.2. Porcine IPEC-J2 cells

The thirty-second passage of IPEC-J2 cells was kindly provided by Dr. Helen Bershneider at the University of North Carolina, and they were passaged 7 more times in our laboratory. In this study, the IPEC-J2 cells were further passaged up to 18 times (total passages 40–58) before use. Virus was inoculated onto 3–4 day-old confluent cell monolayers. The cells were propagated and passaged in the following growth medium: Dulbecco's modified eagle medium/F12 (DMEM/F12) (Gibco, USA) supplemented with 5% fetal bovine serum (FBS), 1% penicillin/streptomycin (Gibco), 1% insulin-transferrin-sodium selenite (Roche), and 5 ng/ml of human epidermal growth factor (Invitrogen), as recommended by Dr. Helen Bershneider.

2.3. Infection of IPEC-J2 cells with PDCoV

The cell culture conditions tested to infect IPEC-J2 cells with PDCoV OH-FD22-P8 during each passage of the virus are described in detail in the Results section. During the 1st [multiplicity of infection (MOI), 2.5] to the 2nd passage of the virus, they were as follows: Washing of cells with maintenance medium (DMEM/F12 supplemented with 1% penicillin/streptomycin) (MMT) twice to remove FBS, virus adsorption for one hour, and then washing (with MMT) once and the addition of MMT with 10 μg/ml of trypsin (Gibco). During the 3rd to 5th serial passage of OH-FD22-P8 virus (estimated MOI, 0.1 for the 4th and 5th passages), however, the wash steps were omitted after virus adsorption. Viral CPE was monitored frequently in the inoculated IPEC-J2 cells.

2.4. Periodic-Acid-Schiff or immunofluorescent staining for the detection of the neutral sialylated mucin, serotonin, or leucine-rich repeat-containing G protein-coupled receptor 5 in IPEC-J2 cells

Prior to the infection assays, we attempted to confirm that no other types of cells were present in the IPEC-J2 cells, such as the mucus-secreting goblet cells or the neutrotransmitter serotonin-secreting enterochromaffin cells, and also tested if the IPEC-J2 cell monolayers express leucine-rich repeat-containing G protein-coupled receptor 5 (LGR5) (intestinal stem cell marker) antigen by Periodic-Acid-Schiff (PAS) or immunofluorescent (IF) staining at post-inoculation hour (PIH) 24, 48, and 72. IPEC-J2 cells were fixed with 100% ethanol at 4 °C overnight and tested by IF staining, as described previously (Hu et al., 2015; Jung et al., 2015a, 2016), for the detection of serotonin or LGR5 antigen, using monoclonal antibodies against human serotonin or human LGR5 (Novus Biologicals, Littleton, CO, USA). Monoclonal antibodies were diluted 1 in 50 in phosphate-buffered saline. PAS staining was used for the detection of the neutral sialylated mucin-secreting goblet cells, according to the manufacturer's instructions and as described previously (Jung and Saif, 2017).

2.5. Analysis of PDCoV RNA or infectious virus titers in cell culture supernatants

Cell culture supernatants were collected from PDCoV-inoculated and non-inoculated IPEC-J2 cells at the time-points as indicated in the Results section. The RNA was extracted from 200 μl of centrifuged (2000 × *g* for 30 min at 4 °C) cell culture supernatants using the MagMAX Viral RNA Isolation Kit (Applied Biosystems, Foster City, CA, USA) according to the manufacturer's instructions. PDCoV RNA titers in cell culture supernatants were determined, as described previously (Jung et al., 2015b). Infectious-virus titration was conducted by a TCID50 assay, as described previously (Hu et al., 2015). IPEC-J2 cells were seeded into 96-well plates, and after confluence, the monolayers were washed once with MMT. One hundred microliters of 10-fold dilutions of PDCoV were inoculated onto the cell monolayers in eight replicates per dilution. After virus adsorption for one hour, another 100 μl of MMT with 10 μg/ml of trypsin was added to each well. Viral CPE was monitored daily for 4 to 6 days, and IF staining was also done for the detection of PDCoV antigen in IPEC-J2 cells as described below. Virus titers were calculated by using the Reed-Muench method and expressed as $TCID_{50}$ per ml.

2.6. Immunofluorescent staining for the detection of PDCoV antigen in IPEC-J2 cells

When PDCoV-inoculated IPEC-J2 cells showed more than 50% CPE, they were fixed with 100% ethanol at 4 °C overnight. The PDCoV-infected cells were prepared in duplicate and tested by IF staining for the detection of PDCoV antigen, using hyperimmune Gn pig antiserum against PDCoV OH-FD22 strain, as described previously (Jung et al., 2015b; Jung et al., 2016). Trypsin (10 μg/ml) alone-treated IPEC-J2 cells were tested as negative controls for IF staining.

2.7. Terminal deoxynucleotidyl transferase-mediated dUTP nick end labelling (TUNEL) assay in IPEC-J2 cells

The IF-stained IPEC-J2 cells were prepared as described above and evaluated by a TUNEL assay kit (Roche Applied Science, Mannheim, Germany) for apoptosis according to the manufacturer's instructions and as described previously (Jung et al., 2016). The IF-stained IPEC-J2 cells were double-stained by TUNEL assay (Jung et al., 2016). Trypsin

(10 μg/ml) alone-treated IPEC-J2 cells were also tested as negative controls for the TUNEL assay.

2.8. Experimental infection of gnotobiotic pigs with the IPEC-J2 cell culture-passaged PDCoV

Six Large White × Duroc crossbred Gn pigs were acquired by hysterectomy from a pregnant sow obtained from a PDCoV- and PEDV-free, specific-pathogen-free (confirmed by history and seronegative sows; lack of qRT-PCR-positive fecal samples) swine herd of The Ohio State University. The SPF herd was seronegative for antibodies to porcine reproductive and respiratory syndrome virus, porcine respiratory coronavirus, transmissible gastroenteritis virus and porcine circovirus type 2. Six 10-day-old Gn piglets were randomly assigned to one of two groups: PDCoV-inoculated (n = 2; pigs 1 and 2) and mock-inoculated (n = 4; pigs 3–6). Pigs were inoculated orally with 2 ml [8.7 $\log_{10}$ genomic equivalents (GE) per pig] of the IPEC-J2 cell culture-passaged PDCoV OH-FD22-P8-I-P4 [passage 4 in IPEC-J2 cells (P4); 8.4 $\log_{10}$ GE/ml], or mock inoculated with MEM. After PDCoV inoculation, the pigs were monitored frequently for clinical signs. PDCoV-inoculated and the negative control pigs were monitored for fecal virus shedding and viremia by qRT-PCR at post-inoculation days (PID) 1 to 5 and then euthanized for pathological examination at PID 5. However, the negative control pigs 4–6 were euthanized at PID 3 to establish other immunologic assays using mononuclear cells isolated from the small intestine. Diarrhea was assessed by scoring fecal consistency. Fecal consistency was scored as follows: 0 = solid; 1 = pasty; 2 = semi-liquid; 3 = liquid, with scores of 2 or more considered diarrheic. The Institutional Animal Care and Use Committee (IACUC) of The Ohio State University approved all protocols related to the animal experiments in this study.

2.9. Analysis of PDCoV RNA titers in fecal and serum samples

Rectal swabs and serum samples were collected from the 2 PDCoV-inoculated and 4 mock-inoculated Gn pigs daily at PID 1–5 and twice at PIDs 1, and 3 or 5, respectively. Two rectal swabs were suspended in 4 ml MEM. The RNA was extracted from 200 μl of the centrifuged (2000 × g for 30 min at 4 °C) fecal suspensions using the Mag-MAX Viral RNA Isolation Kit (Applied Biosystems, Foster City, CA, USA) according to the manufacturer's instructions. PDCoV RNA titers in rectal swab fluids and serum samples were determined as described previously (Jung et al., 2015b).

2.10. Gross and histological analysis and IF staining for the detection of PDCoV antigen

Small [duodenum, middle (mid-location of the small intestine (duodenum to ileum) dissociated from the mesentery), and ileum] and large (cecum/colon) intestinal tissues were examined grossly and histologically in the PDCoV-inoculated pigs 1–2 and mock-inoculated pig 3 at PID 5. Intestinal tissues were tested by IF staining for the detection of PDCoV antigen using the hyperimmune Gn pig antiserum against PDCoV OH-FD22 strain, as described previously (Jung et al., 2015b). PDCoV antigen-positive scores were computed by the number of IF-positive cells in the intestinal section, as described previously (Jung et al., 2014), as follows: +/- (few but clearly positive), < 1% of villous epithelial cells showed staining; + (low), 1%–29% of villous epithelial cells showed staining; + + (moderate), 30%–59% of villous epithelial cells showed staining; + + + (high), 60%–100% villous epithelial cells showed staining; and – (negative), no cells showed staining. Mean ratios of jejunal villous height to crypt depth (VH:CD) were calculated, as described previously (Jung et al., 2015a).

2.11. Analysis of innate and pro-inflammatory cytokine levels in IPEC-J2 cell culture supernatants and serum samples

The levels of IFNα, IL-6, IL-12, IL-22, and TNFα were quantitated by ELISA in the cell culture supernatants (for IFNα, IL-6, and TNFα) or the serum samples collected from the two PDCoV-inoculated Gn pigs 1–2 and the four mock-inoculated Gn pigs 3–6 at PID 1, as described previously (Annamalai et al., 2015; Azevedo et al., 2006; Chattha et al., 2013). Briefly, Nunc Maxisorp 96-well plates were coated with anti-porcine IL-6 (0.75 μg/ml, goat polyclonal antibody), anti-porcine IL-12 (0.75 μg/ml, goat polyclonal antibody), anti-porcine IFNα (2.5 μg/ml, clone K9) (R&D systems, Minneapolis, MN), anti-porcine IL-22 (2.0 μg/ml, rabbit polyclonal antibody), and anti-porcine TNFα (1.5 μg/ml, goat polyclonal antibody) (Kingfisher biotech, Saint Paul, MN) overnight at 4 °C or 37 °C (for IFN-α only). Biotinylated anti-porcine IL-6 (0.1 μg/ml, goat polyclonal antibody), anti-porcine IL-12 (0.2 μg/ml, goat polyclonal antibody), anti-porcine IFNα (3.75 μg/ml, clone F17) (R&D systems, Minneapolis, MN), anti-porcine IL-22 (0.5 μg/ml, rabbit polyclonal antibody), and anti-porcine TNFα (0.4 μg/ml, goat polyclonal antibody) (Kingfisher biotech, Saint Paul, MN) were used as detection antibodies. The porcine IFN-α detection antibody was biotinylated using a commercial kit, as described previously (Chattha et al., 2013). Plates were developed and cytokine concentrations were calculated, as previously described (Annamalai et al., 2015; Azevedo et al., 2006). The samples were tested in duplicate, and cytokine levels were expressed as the mean values. Detection limits of our ELISA were 1 pg/ml for IFNα and IL-12, 4 pg/ml for TNFα and IL-22, and 16 pg/ml for IL-6, respectively.

3. Results

3.1. IPEC-J2 cells appeared to consist mostly of intestinal absorptive (non-secretory) villous enterocytes

IPEC-J2 cells are known to consist mostly of intestinal columnar epithelial cells (absorptive enterocytes) (Brosnahan and Brown, 2012; Vergauwen, 2015). After trypsinization, the detached IPEC-J2 cells were spin down by centrifugation; however, the pelleted cells appeared more adhesive and clumped, relative to immortalized cell lines of epithelial cell origin. Therefore, prior to the infection assays using the cells, we attempted to confirm that no other types of cells were present, such as spindle-shaped (or fusiform) smooth muscle cells constituting connective tissue, the mucus-secreting goblet cells, or the neurotransmitter serotonin-secreting enterochromaffin cells in the IPEC-J2 cell monolayers by light microscopy (or PAS staining) or IF staining at PIH 24, 48, and 72 (different stages of cell differentiation). These types of cells are anatomically located in the lamina propria (smooth muscle cell), or villous (goblet cell) or crypt (enterochromaffin cell) epithelium of the mid-jejunum, from which the IPEC-J2 cells were isolated (Brosnahan and Brown, 2012; Vergauwen, 2015). By light microscopic examination, there were no fusiform (or fibrous) cells, but only polygonal, homogenous cells at PIH 24–72. By IF, there were also neither goblet cells positive for Periodic-Acid-Schiff staining, nor enterochromaffin cells positive for serotonin in the IPEC-J2 cell monolayers at PIH 24–72. Consistent with the previous reports (Brosnahan and Brown, 2012; Vergauwen, 2015), the IPEC-J2 cells appeared to consist mostly of intestinal absorptive (non-secretory) villous enterocytes. However, a recent study reported that the non-homogeneity of the IPEC-J2 cells that they observed might be associated with little or no susceptibility of the cells to PEDV infection, and that only the subcloned IPEC-J2 cells became susceptible to PEDV infection (Zhang et al., 2018). Nevertheless, it is critical to note that IPEC-J2 cells have been infected successfully with PEDV, as reported previously (Lin et al., 2017; Shi et al., 2017; Zhao et al., 2014). The IPEC-J2 cells also showed the ability to continuously differentiate into daughter cells, as also was supported by IF staining, showing large numbers of IPEC-J2 cells

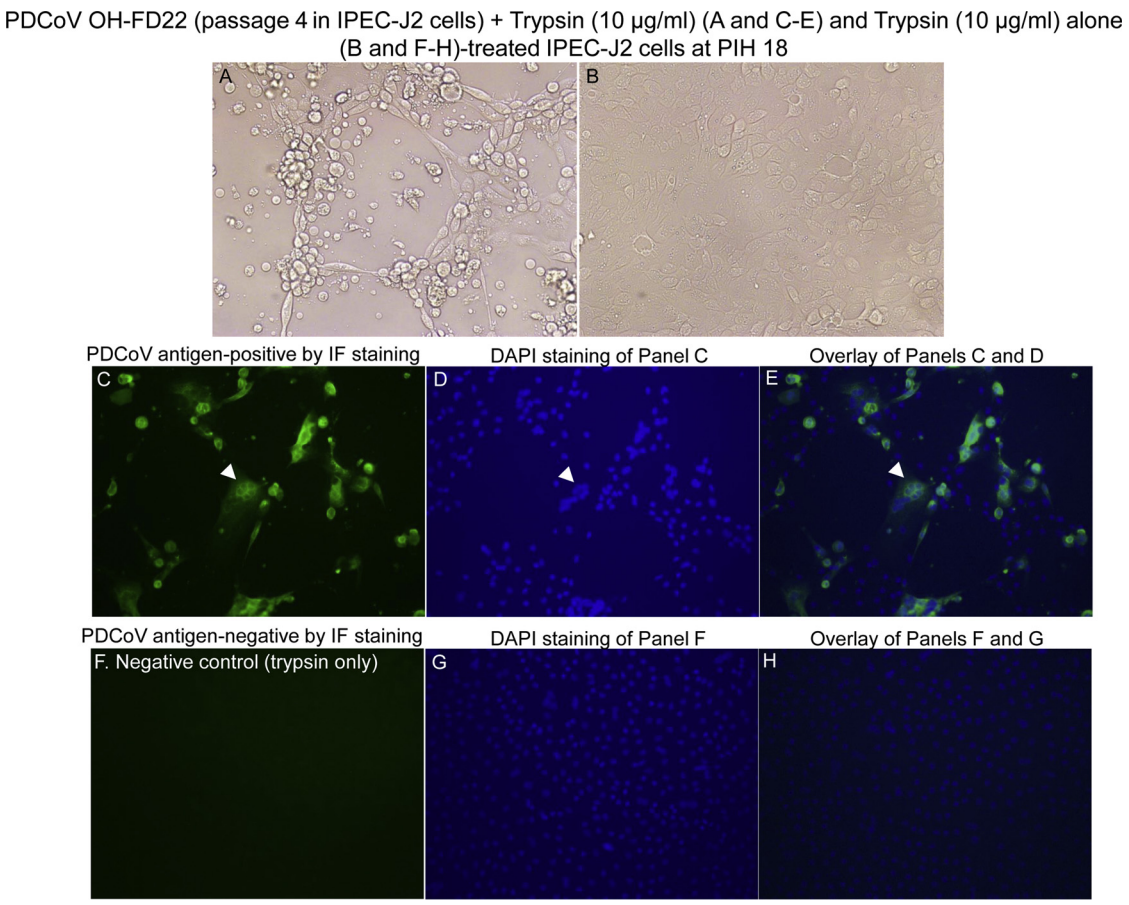

Fig. 1. Cytopathic effects (CPE) and localization of PDCoV antigens by immunofluorescent (IF) staining in the IPEC-J2 cells inoculated with the PDCoV strain OH-FD22 during the 4th serial passage, and supplemented with 10 μg/ml of trypsin in the cell culture medium. (A) PDCoV OH-FD22-inoculated IPEC-J2 cells at post-inoculation hour (PIH) 18, showing CPE that consists of enlarged, rounded, and densely granular cells that occurred singly or in clusters, often forming cell clumps, followed by cell shrinkage and detachment. (B) PDCoV-uninoculated IPEC-J2 cells supplemented with 10 μg/ml of trypsin showing normal cells. (C) IF staining of the inoculated IPEC-J2 cells at PIH 18, showing that the enlarged, rounded, and clustered cells are positive for PDCoV antigen (green staining). (D) Blue-fluorescent 4′, 6-diamidino-2-phenylindole dihydrochloride (DAPI) staining of Panel C to counterstain nuclear DNA. (E) Overlay of Panels C and D. Note that the entire clustered cells positive for PDCoV antigen (arrowheads) appeared to be syncytial or multinucleated cells. (F) IF staining of PDCoV-uninoculated, trypsin (10 μg/ml)-treated IPEC-J2 cells at PIH 18, showing no cells positive for PDCoV antigen. (G) DAPI staining of Panel F. (H) Overlay of Panels F and G. Original magnification, all ×200.

positive for the intestinal stem cell (or crypt cell) marker, LGR5 at PIH 24–72 (Supplemental Fig. S1).

3.2. Supplemental trypsin in the cell culture medium was beneficial for propagation of PDCoV in the IPEC-J2 cells

In LLC-PK cells, supplemental trypsin in the cell culture medium contributed to a significant increase in PDCoV titers after several passages in LLC-PK cells, accompanied by CPE, compared with non-trypsin supplemented cell cultures (Hu et al., 2015). Furthermore, supplemental trypsin (5 μg/ml) in the cell culture medium also led to the successful growth of PEDV in IPEC-J2 cells (Shi et al., 2017). Based on these observations, prior to the supplementation of trypsin in the IPEC-J2 cell culture medium, we investigated if virus titers differ between PDCoV-inoculated IPEC-J2 cells supplemented with lower vs. higher concentrations of trypsin. An MOI of 2.5 of PDCoV OH-FD22-P8 was used for inoculation of IPEC-J2 cell monolayers in 6-well plates supplemented with two different concentrations of trypsin (2.5 vs. 10 μg/ml) in the cell culture medium. Negative controls included cells treated with no virus but trypsin. Washing was done after virus adsorption for 1 h, as described previously (Hu et al., 2015), and 2 ml of maintenance medium supplemented with trypsin was added. Cell culture supernatants were collected to analyze PDCoV RNA titers by qRT-PCR at PIH 20, 42, and 72. PDCoV RNA titers in trypsin (10 μg/ml)-treated, PDCoV-inoculated IPEC-J2 cells were 9.5 $\log_{10}$ GE/ml, 9.6 $\log_{10}$ GE/ml, and 9.8 $\log_{10}$ GE/ml at PIH 20, 42, and 72, respectively, whereas viral RNA titers in the lower trypsin (2.5 μg/ml)-treated, PDCoV-inoculated IPEC-J2 cells were lower (8.5 $\log_{10}$ GE/ml, 9.1 $\log_{10}$ GE/ml, and 9.3 $\log_{10}$ GE/ml at PIH 20, 42, and 72, respectively). However, neither of the PDCoV-inoculated, trypsin-treated groups showed CPE at PIH 20-72. None of the cell culture supernatants from the PDCoV-uninoculated, trypsin-treated negative controls were positive for PDCoV RNA at PIH 20-72. Based on these observations, the supplemental trypsin in the cell culture medium appeared to be beneficial for the growth of PDCoV in the IPEC-J2 cells. Therefore, maintenance medium was supplemented consistently with 10 μg/ml of trypsin during further serial passages of PDCoV in the IPEC-J2 cells. However, our study did not define either the optimal concentration of trypsin for growth of PDCoV in the IPEC-J2 cells, or the maximum concentration of trypsin tolerated by the IPEC-J2 cells.

3.3. Cytopathic effects were first identified during the 3rd serial passage of PDCoV OH-FD22-P8 in the IPEC-J2 cells

The PDCoV OH-FD22-P8 strain passaged in IPEC-J2 cells with the highest viral RNA titer in the cell culture supernatant (OH-FD22-P8-I-P1) after the 1st passage was passaged continuously in the IPEC-J2 cells supplemented with 10 μg/ml of trypsin in the cell culture medium. For

the 2nd passage, like the 1st passage, no CPE was observed by 4–5 days after virus inoculation. Therefore, for the 3rd passage of the virus, the following modifications in the procedure were tested to improve PDCoV growth and observe CPE: i) omitting washing of the cells after virus adsorption or ii) omitting removal of the inoculum. When the wash step was omitted, inoculated cells showed no CPE until PIH 24, but at PIH 48, most of cells were detached (> 90%) and most of the detached cells appeared rounded and shrunken. The PDCoV RNA titer of the cell culture supernatant was 10.5 $\log_{10}$ GE/ml at PIH 48. On the other hand, when the removal of the inoculum was omitted, no CPE was found for 4 days after inoculation. However, a high PDCoV RNA titer of 9.0 $\log_{10}$ GE/ml was still observed in the cell culture supernatant at PIH 48. These observations support the necessity for optimal trypsin concentrations in the MMT for PDCoV-induced CPE in IPEC-J2 cells. For continuous serial passages, the wash step was also omitted.

3.4. Cytopathic effects and PDCoV antigen were identified in PDCoV-inoculated IPEC-J2 cells

An estimated MOI of 0.1 of the OH-FD22-P8-I-P3 (passage 3 in IPEC-J2 cells, 5×10^6 $TCID_{50}$/ml) was used as inoculum for the 4th passage in IPEC-J2 cells. At PIH 18, PDCoV-inoculated IPEC-J2 cells treated with trypsin (10 μg/ml) exhibited CPE that consisted of enlarged, rounded, and densely granular cells that occurred singly or in clusters, often forming cell clumps, followed by cell shrinkage and detachment (Fig. 1A and B). Large numbers of the single or clustered cells that showed CPE at PIH 18 were positive for PDCoV antigen by IF staining (Fig. 1C–E), whereas no IF-positive cells were found in the PDCoV-uninoculated, trypsin-treated negative controls (Fig. 1F–H). By IF staining, occasionally the entire cluster of cells were positive for PDCoV antigen, and they resembled syncytial or multinucleated cells (Fig. 1C–E).

3.5. Double IF and TUNEL staining revealed that PDCoV-infected IPEC-J2 cells may not undergo apoptosis

By double IF and TUNEL staining at PIH 18 when more than 50% CPE was observed, most or large numbers of the PDCoV antigen-positive IPEC-J2 cells failed to show TUNEL-positive signals (Fig. 2A–D), although most of them showed CPE (enlarged and round cells). TUNEL-positive signals were confirmed to be in only a few PDCoV antigen-positive IPEC-J2 cells (Fig. 2E–H); moreover, in the same microscopic areas positive for TUNEL, most or large numbers of the PDCoV antigen-positive IPEC-J2 cells did not show TUNEL-positive signals (Fig. 2H), indicative of little or no positive correlation of PDCoV antigens with TUNEL signals. The TUNEL-positive signals were characterized by small numbers of multiple small, round, dense, fragmented, red staining clusters (Fig. 2G), which appeared to be fragmentation of the nucleus into multiple nuclear membrane-bound chromatin (apoptotic) bodies. The PDCoV-uninoculated, trypsin-treated IPEC-J2 cells showed no CPE, IF- or TUNEL-positive staining. Overall, the nuclei of IPEC-J2 cells infected with PDCoV did not undergo fragmentation, indicating that PDCoV-infected IPEC-J2 cells may not undergo apoptosis, but rather necrosis, similar to necrotic cell death of infected enterocytes *in vivo* (Jung et al., 2016).

3.6. PDCoV titers and pro-inflammatory (IL-6) cytokine levels increased in parallel (through PIH 72) in cell culture supernatants of the IPEC-J2 cells

An estimated MOI of 0.1 of the OH-FD22-P8-I-P4 (passage 4 in IPEC-J2 cells, 1×10^6 $TCID_{50}$/ml) was inoculated in duplicate onto IPEC-J2 cell monolayers (2 × T75 flasks) for the 5th passage, alongside a PDCoV-uninoculated, trypsin-treated negative control (1 × T75 flask). After virus adsorption, the wash step was omitted, and 15 ml of trypsin supplemented cell culture medium was added. The cell culture supernatants (1 ml per time-point) were harvested at PIH 7, 24, 31, 48, 72, and 96. Viral CPE such as round and detached cells were observed at PIH 24, the CPE increased progressively (up to 70% CPE) until PIH 96, but complete cell detachment was not observed until PIH 96. The cell culture supernatants were harvested, centrifuged (1000 × g for 10 min at 4 °C) and stored at −70 °C for subsequent testing. The mean infectious titers from the duplicate samples began to increase at PIH 24, compared with PIH 7, then elevated progressively and peaked at PIH 72, and decreased at PIH 96 (Fig. 3A). Similarly, mean IL-6 concentrations from the duplicate samples increased by 6.2-fold at PIH 48, compared with the PDCoV-uninoculated, trypsin-treated negative control, and then increased progressively and peaked (by 129-fold compared with the PDCoV-uninoculated, trypsin-treated negative control) at PIH 96 (Fig. 3B). The levels of the pro-inflammatory TNFα and innate IFNα cytokines in the cell culture supernatants of PDCoV-inoculated and non-inoculated cells at PIH 7–96 remained under the detection limits (1 pg/ml and 4 pg/ml for IFNα and TNFα, respectively).

3.7. IPEC-J2 cell culture-passaged PDCoV (OH-FD22-P8-I-P4) was enteropathogenic in 10-day-old gnotobiotic pigs

Because of the increased IL-6 observed in the PDCoV-infected IPEC-J2 cells *in vitro,* as well as the lack of information on serum cytokine profiles during an acute PDCoV infection, we studied the enteropathogenicity of the IPEC-J2 cell culture-passaged PDCoV (OH-FD22-P8-I-P4) in Gn pigs and the innate and pro-inflammatory cytokines induced in their sera. At PID 1, PDCoV-inoculated pigs 1 and 2 exhibited watery diarrhea, accompanied by vomiting, which (but not vomiting) persisted throughout the experiment (PID 5), whereas the 4 PDCoV-uninoculated control pigs did not show any clinical signs for the experimental period (Table 1). The PDCoV-inoculated pigs 1 and 2 and negative control pigs 3–6 were monitored for viral RNA titers in the feces and sera and then euthanized at PID 5 for pathological examination. The results are summarized in Table 1. At PID 1–5, by qRT-PCR, PDCoV-inoculated Gn pigs 1 and 2 had moderate to high viral RNA titers in the feces, ranging from 6.7 to 10.0 $\log_{10}$ GE/ml with peak titers of 9.9–10.0 $\log_{10}$ GE/ml at PID 1, whereas no negative control pigs had detectable viral RNA (< 4.6 $\log_{10}$ GE/ml) in the feces during the experimental period. PDCoV-inoculated Gn pigs 1 and 2 also had low viral RNA titers in serum at PID 1 and 5, ranging from 4.0 to 5.0 $\log_{10}$ GE/ml, whereas no negative control pigs had detectable viral RNA (< 3.6 $\log_{10}$ GE/ml) in the serum samples at PID 1, 3, and 5.

At PID 5, the PDCoV-inoculated Gn pigs 1 and 2 exhibited gross lesions characterized by thin and transparent intestinal walls and luminal accumulation of large amounts of watery liquid in the small (but with lack of lesions in the duodenum to proximal jejunum close to the pylorus) (Fig. 4A) and large intestine. No gross lesions were evident in the other organs of the PDCoV-inoculated Gn pigs 1 and 2 and negative control pig 3. Histologically, the duodenum of PDCoV-inoculated Gn pigs 1 and 2 showed normal mucosa, submucosa, and serosa. However, their mid-jejunum and ileum showed diffuse, severe villous atrophy (Fig. 4B–E), as jejunal villous height: crypt depth (VH:CD) ratios ranged from 1.3 to 1.4 compared with 5.7 in the negative control pig 3 (Fig. 4B and C; Table 1). No histologic lesions were evident in the large intestine and other organs of the PDCoV-inoculated Gn pigs 1 and 2 and the negative control. At PID 5, PDCoV antigens were found mostly in the villous epithelial cells, but not the crypt epithelial cells (Fig. 4D and 4E). At PID 5, PDCoV-inoculated Gn pigs 1 and 2 showed moderate to high numbers of PEDV antigen-positive cells in the mid-jejunal epithelium (Fig. 4D), low numbers of PEDV antigen-positive cells in the duodenal and ileal epithelium (Fig. 4E), and a few positive cells in the colon. Low numbers of PDCoV antigen-positive cells were also detected in the Peyer's patches (Fig. 4E). No PDCoV antigen-positive cells were detected in the intestine of the negative control pig 3.

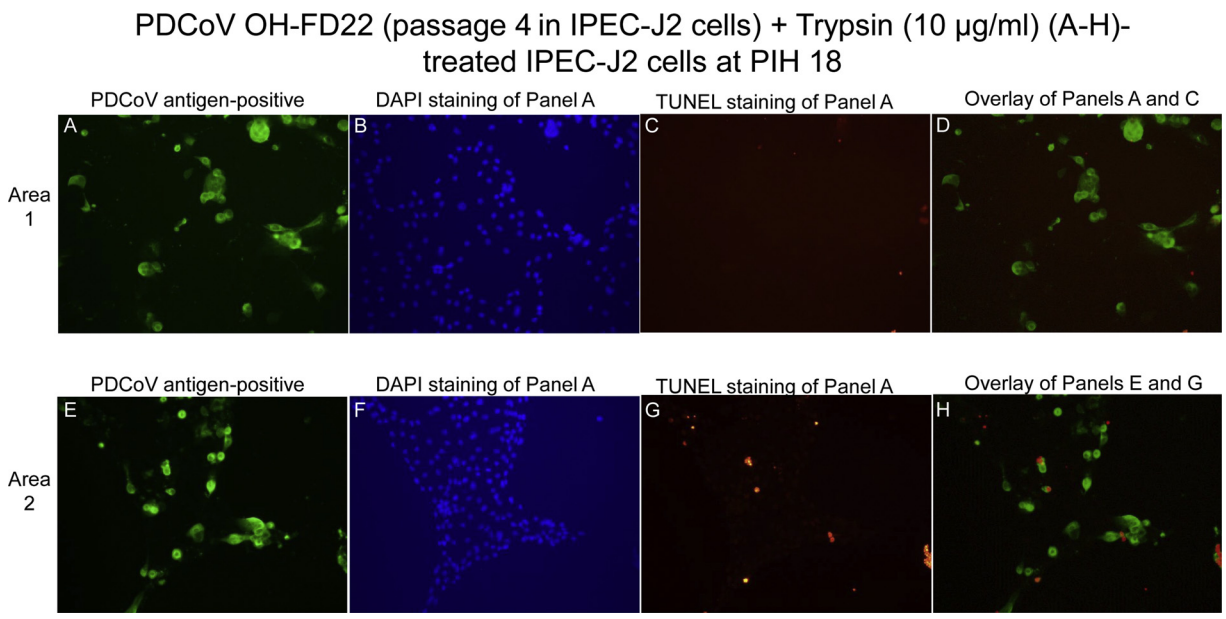

Fig. 2. Localization of PDCoV antigens by immunofluorescent (IF) staining and apoptotic cells by a TUNEL assay in the IPEC-J2 cells inoculated with the PDCoV strain OH-FD22 during the 4th serial passage, and supplemented with 10 μg/ml of trypsin in the cell culture medium. (A) IF staining of the inoculated IPEC-J2 cells at post-inoculation hour (PIH) 18, showing that the enlarged, rounded, and clustered cells are positive for PDCoV antigen (green staining). (B) Blue-fluorescent 4′, 6-diamidino-2-phenylindole dihydrochloride (DAPI) staining of Panel A. (C) Double TUNEL staining of Panel A, showing that most of the cytopathic effect (CPE)- and PDCoV antigen-positive cells are TUNEL (intranuclear red staining)-negative. (D) Overlay of Panels A and C, showing that few PDCoV antigen-positive cells are TUNEL-positive (intranuclear red staining); however, most of the PDCoV antigen-positive IPEC-J2 cells did not show TUNEL-positive signals, indicative of no positive correlation of PDCoV antigens with TUNEL signals. (E) IF staining of the inoculated IPEC-J2 cells at PIH 18 (other microscopic area that differs from Panels A–D), showing that the enlarged, rounded, and clustered cells are positive for PDCoV antigen (green staining). (F) DAPI staining of Panel A. (G) Double TUNEL staining of Panel A, showing that a number of the CPE- and PDCoV antigen-positive cells are TUNEL (intranuclear red staining)-negative. (H) Overlay of Panels A and C, showing that a few PDCoV antigen-positive cells are TUNEL-positive (intranuclear red staining); however, most of the PDCoV antigen-positive IPEC-J2 cells did not show TUNEL-positive signals, indicative of little or no positive correlation of PDCoV antigens with TUNEL signals. Original magnification, all ×200. TUNEL, terminal deoxynucleotidyl transferase-mediated dUTP nick end labelling.

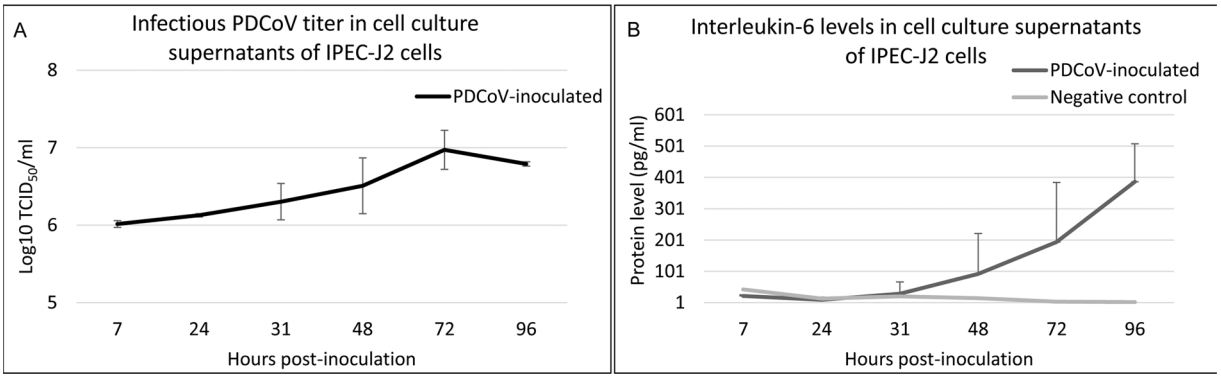

Fig. 3. Increased viral titers (A) and pro-inflammatory (IL-6) cytokine levels (B) in the cell culture supernatants of IPEC-J2 cells during the 5th serial passage of PDCoV OH-FD22. An estimated MOI of 0.1 of an OH-FD22-P8-I-P4 (passage 4 in IPEC-J2 cells) was inoculated in duplicate onto IPEC-J2 cell monolayers (2 × T75 flasks) for the 5th passage, alongside a PDCoV-uninoculated, trypsin-treated negative control (1 × T75 flask). After virus adsorption, the wash step was omitted, and 15 ml of trypsin supplemented cell culture medium was added. The cell culture supernatants (1 ml per time-point) were harvested at PIHs 7, 24, 31, 48, 72, and 96. The cell culture supernatants harvested were centrifuged (1000 × g for 10 min at 4 °C) and stored at −70 °C until virus quantification by a $TCID_{50}$ assay (A) and cytokine quantification by ELISA (B). The samples were tested in duplicate, and cytokine levels or infectious virus titers were expressed as the mean values.

3.8. IPEC-J2 cell culture-passaged PDCoV induced systemic innate and pro-inflammatory cytokine responses at PID 1 in inoculated gnotobiotic pigs

Serum innate (IFNα and IL-22) cytokines, which are known to play a role in antiviral immune responses (Gimeno Brias et al., 2016; Zhang and Yoo, 2016), and pro-inflammatory (TNFα, IL-6, and IL-12) cytokines were evaluated at PID 1 in the Gn pigs 1–6 to compare with the *in vitro* findings (increased IL-6 in PDCoV-infected IPEC-J2 cells) as well as to investigate whether acute PDCoV infection induces systemic innate and pro-inflammatory cytokine immune responses. Compared with the four uninfected Gn pigs 3–6 at PID 1, in the infected Gn pig 1, serum IFNα and IL-22 were increased by 190-fold and 112-fold, respectively, and serum TNFα, IL-6, and IL-12 were each increased by 4-fold, 4-fold, and 4-fold (Table 2). Similarly, compared with the four uninfected Gn pigs 3–6 at PID 1, in the infected Gn pig 2, serum IFNα and IL-22 increased by 390-fold and 33-fold, respectively, and serum TNFα, IL-6, and IL-12 were each increased by 4-fold, 3-fold, and 3-fold (Table 2). Although statistical analysis was not done due to too few animals in the infected group, the data clearly indicate that infected Gn pigs exhibited pronounced systemic innate and to a lesser extent, pro-inflammatory cytokine responses to acute PDCoV infection.

Table 1
Summary of clinical signs, viral RNA titers in the feces and serum samples, and histopathologic and immunofluorescent (IF) staining results from 10-day-old gnotobiotic pigs inoculated orally with 8.7 log_{10} GE/pig of the IPEC-J2 cell culture-passaged PDCoV (OH-FD22-P8-I-P4) or mock at post-inoculation day (PID) 1 to 5.

Group	Pig no.		Viral RNA titer, log_{10} GE/mL, by PID[a]						Mean jejunal VH:CD ratio (SD)[c]	PDCoV antigen detection by IF staining in FFPE tissues[c,d]			
			0	1	2	3	4	5		D	MJ	I	C
PDCoV-inoculated	1	Feces (score)[b]	< 4.6 (1)	10.0 (3)	6.7 (3)	7.3 (3)	7.1 (3)	7.9 (3)	1.4 (0.3)	+	+ + or + + +	+	±
		Serum	< 3.6	4.4	.	.	.	4.4					
	2	Feces (score)	< 4.6 (1)	9.9 (3)	8.0 (3)	7.6 (3)	6.9 (3)	9.3 (3)	1.3 (0.2)	+	+ + +	+	±
		Serum	< 3.6	4.0	.	.	.	5.0					
Mock-inoculated	3 (15[e])	Feces (score)	< 4.6 (0)	< 4.6 (0)	< 4.6 (0)	< 4.6 (0)	< 4.6 (0)	< 4.6 (0)	5.7 (0.4)	−	−	−	−
		Serum	< 3.6	< 3.6	.	.	.	< 3.6					
	4 (13[e])	Feces (score)	< 4.6 (0)	< 4.6 (0)	< 4.6 (0)	< 4.6 (0)	.	.	ND	ND			
		Serum	< 3.6	< 3.6	.	< 3.6	.	.					
	5 (13[e])	Feces (score)	< 4.6 (0)	< 4.6 (0)	< 4.6 (0)	< 4.6 (0)	.	.	ND	ND			
		Serum	< 3.6	< 3.6	.	< 3.6	.	.					
	6 (13[e])	Feces (score)	< 4.6 (0)	< 4.6 (0)	< 4.6 (0)	< 4.6 (0)	.	.	ND	ND			
		Serum	< 3.6	< 3.6	.	< 3.6	.	.					

GE, genomic equivalent; VH:CD ratio, villous height to crypt depth ratio; SD, standard deviation; FFPE, formalin-fixed, paraffin-embedded; D, duodenum; MJ, mid-jejunum; I, ileum; C, colon; ND, not determined.

[a] Detected by real-time reverse transcription PCR with a detection limit of 4.6 log_{10} GE/ml for fecal samples and 3.6 log_{10} GE/ml for serum samples.

[b] Fecal consistency was scored as follows: 0 = solid; 1 = pasty; 2 = semi-liquid; 3 = liquid, with scores of 2 or more considered diarrheic.

[c] Euthanasia was done at PID 5.

[d] Detected by IHC in multiple tissue sections, resulting in a range of IF score. +/- (few), < 1% of villous epithelial cells showed staining; + (low), 1%–29% of villous epithelial cells showed staining; + + (moderate), 30%–59% of villous epithelial cells showed staining; + + + (high), 60%–100% villous epithelial cells showed staining; and -, no cells showed staining.

[e] Pig age (days) at euthanasia. Note that the negative control pigs 4–6 were euthanized at PID 3 to establish other immunologic assays using mononuclear cells isolated from the small intestine.

4. Discussion

Based on our data, IPEC-J2 cells are susceptible to infection with PDCoV, like for the other enteric CoVs, PEDV and TGEV (Guo et al., 2016; Lin et al., 2017; Shi et al., 2017; Xia et al., 2017; Zhao et al., 2014). Compared with LLC-PK or ST cells, our previous study revealed no or less susceptibility of IPEC-J2 cells to PDCoV infection using feces or intestinal contents or tissues of PDCoV-infected pigs (Hu et al., 2015). However, our current study verified that PDCoV previously grown in other swine cell cultures such as LLC-PK cells can be propagated and passaged in IPEC-J2 cells. Recently, porcine aminopeptidase N (pAPN) was identified as a major cell entry receptor for PDCoV (Li et al., 2018; Wang et al., 2018; Zhu et al., 2018). Therefore, possible differences in pAPN expression levels among the LLC-PK, ST, and IPEC-J2 cells of swine origin could influence their susceptibility to infection with PDCoV. Supplementation of 10 μg/ml of trypsin and 1% pancreatin in the cell culture maintenance medium for LLC-PK and ST cells, respectively, was essential for both growth and CPE of PDCoV in these two cell lines. Similarly, we found that addition of trypsin to the cell culture maintenance medium also contributed to both growth and CPE of PDCoV in IPEC-J2 cells. It is also noteworthy that of the two modifications in the virus inoculation procedure, i) omitting washing of the cells after virus adsorption or ii) omitting removal of the inoculum, the former method was likely more efficient to improve PDCoV growth and observe CPE in our experimental conditions, compared with the latter and initial (washing of the cells after virus adsorption) methods. The approach of omitting removal of the inoculum was used to isolate PEDV from clinical samples in Vero cells (Hofmann and Wyler, 1988; Oka et al., 2014). The sensitivity of virus isolation was higher than that by the method of washing the cells after virus adsorption (Oka et al., 2014). Even after the virus adsorption procedure ended, the two modifications might have allowed cell-unbound viruses to continue to bind to the cell surface. The cell-unbound viruses might have also underwent proteolysis of the spike protein in the presence of trypsin in the cell culture maintenance medium, resulting in cell entry of PDCoV via the cellular receptor, pAPN, although optimal trypsin concentrations might be needed in the maintenance medium, as mentioned in the Results section 3.3.

By light microscopic examination, CPE observed in the three LLC-PK, ST, and IPEC-J2 cell lines appeared similar, consisting of enlarged, rounded, and densely granular cells that occurred singly or in clusters, followed by cell shrinkage and detachment. In infected LLC-PK or ST cells, CPE might be a result of apoptotic cell death, as reported previously (Jung et al., 2016). Interestingly, however, our current study revealed no positive correlation of PDCoV antigen or CPE with TUNEL signals, unlike PDCoV infection in LLC-PK or ST cells. Our double IF and TUNEL staining demonstrated that most or large numbers of the PDCoV antigen- and CPE-positive IPEC-J2 cells failed to show TUNEL-positive signals. The few TUNEL-positive signals found in the few PDCoV antigen-positive IPEC-J2 cells might be associated with increased IL-6 in PDCoV-infected IPEC-J2 cells or other undefined intrinsic apoptosis pathway inducers (Grunnet et al., 2009; Salguero et al., 2005). Based on these observations, the cell death observed in PDCoV-infected IPEC-J2 cells may not be due to apoptosis, but possibly, necrosis as a result of the cytolytic action(s) of the virus, similar to necrotic cell death observed in PDCoV-infected intestinal villous epithelial cells *in vivo* (Jung et al., 2016).

Our study also revealed that IL-6 increased in PDCoV-infected IPEC-J2 cell culture supernatants at PIH 48–96, as tested by ELISA, concurrent with the increased titers of PDCoV at PIH 24–72. Compared with the PDCoV-uninoculated, trypsin-treated negative control, IL-6 levels in the infected IPEC-J2 cells increased by 6.2- to 129-fold at PIH 48–96, indicating that PDCoV induces this pro-inflammatory cytokine and that IPEC-J2 cells are capable of producing IL-6. The increased IL-6 levels in PDCoV-infected IPEC-J2 cells is similar to the increased mRNA levels of pro-inflammatory cytokines (IL-1β, IL-6, IL-8 and TNFα) in IPEC-J2 cells infected with PEDV (Lin et al., 2017).

To our knowledge, there is no information on serum cytokine responses of pigs to acute PDCoV infection. Therefore, in our study, we inoculated Gn piglets orally with the IPEC-J2 cell culture-passaged PDCoV to define innate and pro-inflammatory cytokine profiles in the sera during the acute stage of infection as well as to confirm the

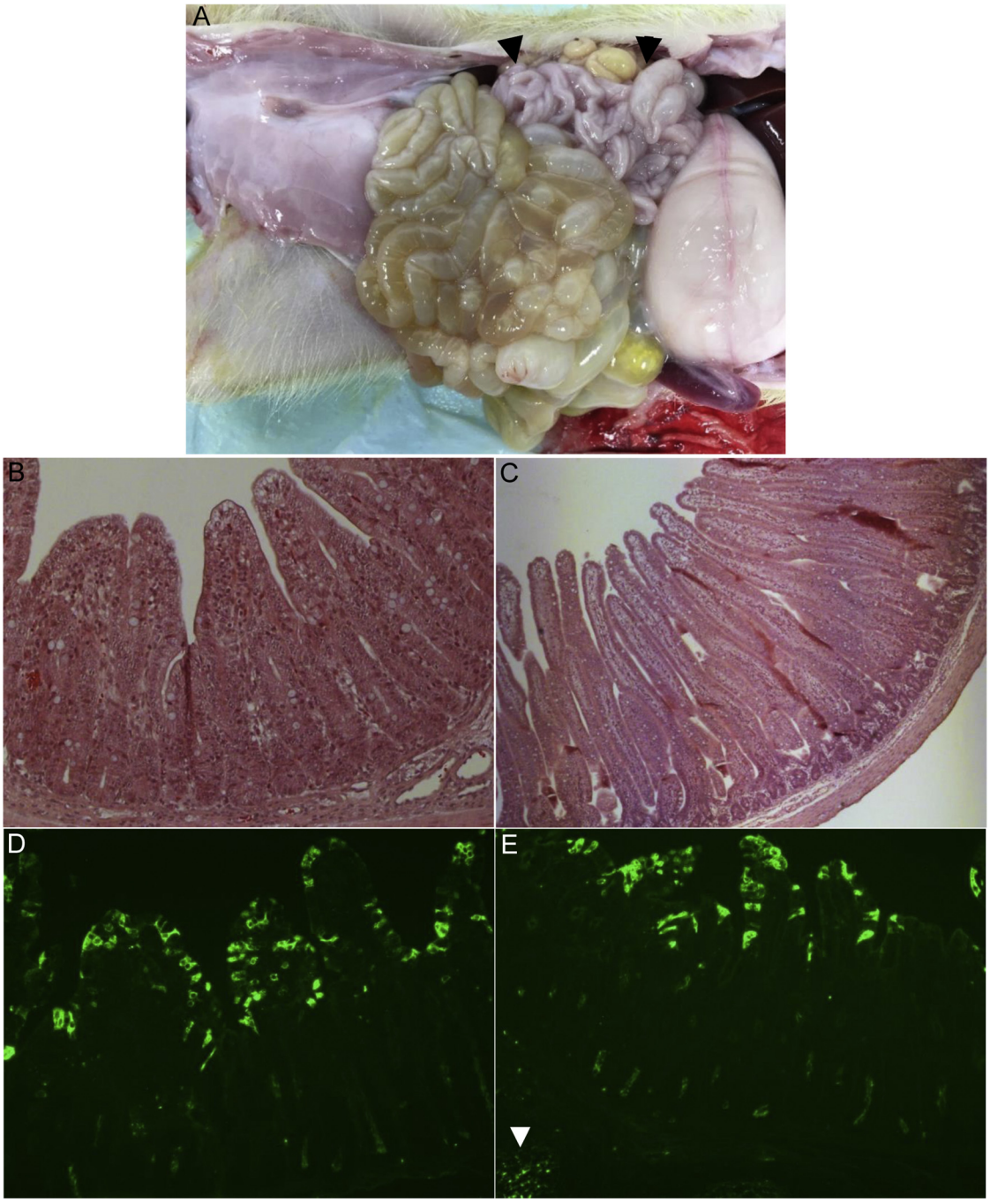

Fig. 4. Gross and histological lesions and detection of PDCoV antigen by immunofluorescent (IF) staining in the intestine of 10-day-old gnotobiotic pigs inoculated orally with the IPEC-J2 cell culture-passaged PDCoV (OH-FD22-P8-I-P4) or mock. (A) Intestine of PDCoV-inoculated pig 1 at post-inoculation day (PID) 5, showing thin and transparent intestinal walls and luminal accumulation of large amounts of watery liquid in the small [but with lack of lesions in the duodenum to proximal jejunum close to the pylorus (arrowheads)] and large intestine. (B) Hematoxylin and eosin-stained mid-jejunum of PDCoV-inoculated pig 1 at (PID) 5, showing severe atrophic enteritis. (C) Hematoxylin and eosin-stained mid-jejunum of mock-inoculated pig 3 at PID 5, showing normal villous epithelium. (D) IF-stained mid-jejunum of PDCoV-inoculated pig 1 at PID 5, showing moderate numbers of PDCoV antigen-positive cells (green color) in the villous epithelium. (E) IF-stained ileum of PDCoV-inoculated pig 1 at PID 5, showing low numbers of PDCoV antigen-positive cells (green color) in the villous epithelium. Note low numbers of PDCoV antigen-positive cells in the Peyer's patch (arrowhead). Original magnification, ×200 (panels B, D, and E) or ×80 (panel C).

enteropathogenicity in pigs. Our study verified the enteropathogenicity of the IPEC-J2 cell culture-passaged PDCoV (OH-FD22-P8-I-P4) in the inoculated Gn pigs 1 and 2, similar to that of the original (wild-type) or LLC-PK cell culture-grown OH-FD22 strain in Gn pigs (Hu et al., 2016; Jung et al., 2015b). The inoculated pigs exhibited watery diarrhea and moderate to high viral RNA titers in the feces (6.7–10.0 $\log_{10}$ GE/ml) at PID 1–5 and severe atrophic enteritis (jejunal VH:CD ratio of 1.3–1.4) at PID 5. Our current study also clearly demonstrated that predominantly innate (IFNα and IL-22) and to a lesser extent, pro-inflammatory (TNFα, IL-6, and IL-12) cytokine levels in the sera of infected Gn pigs during acute PDCoV infection (PID 1) were increased by 33- to 390-fold and 3- to 4-fold, respectively, compared with the corresponding negative control pigs. This observation is similar to increased serum innate (IFNα and IL-22) and pro-inflammatory (IL-6, TNFα, and IL-12) cytokine responses of 9-10-day old, Gn or conventional pigs to acute PEDV infection (Annamalai et al., 2015; Jung, Miyazaki, and Saif,

Table 2
Innate and pro-inflammatory cytokine levels quantitated by ELISA in the sera of 10-day-old gnotobiotic pigs inoculated with the IPEC-J2 cell culture-passaged PDCoV (OH-FD22-P8-I-P4) or mock at post-inoculation day 1.

Group	Pig no.	Clinical signs	Innate[a]		Pro-inflammatory[a]		
			IFNα (pg/ml) (fold increase)	IL-22 (pg/ml) (fold increase)	TNFα (pg/ml) (fold increase)	IL-6 (pg/ml) (fold increase)	IL-12 (pg/ml) (fold increase)
PDCoV-inoculated	1	Watery diarrhea	332[b] (190-fold)	446 (112-fold)	18 (4-fold)	622 (4-fold)	78 (4-fold)
	2	Watery diarrhea	682 (390-fold)	133 (33-fold)	18 (4-fold)	542 (3-fold)	68 (3-fold)
Mock-inoculated	3	None	1	4	4	222	28
	4	None	1	4	4	175	22
	5	None	2	4	5	105	13
	6	None	3	4	4	138	17
	Mean (SD)[c]		2 (1)	4 (0)	4 (1)	160 (50)	20 (6)

[a] The samples were tested in duplicate, and cytokine levels were expressed as the mean values. Detection limits of our ELISA were 1 pg/ml for IFNα and IL-12, 4 pg/ml for TNFα and IL-22, and 16 pg/ml for IL-6, respectively.

[b] Bold numbers, trends toward increased innate (IFNα and IL-22) and pro-inflammatory (TNFα, IL-6, and IL-12) cytokine levels in sera of PDCoV-infected pigs and the fold increases compared with the mean values of the cytokines tested in the four mock-inoculated pigs 3–6.

[c] Although statistical analysis was not done due to too few animals in the infected group, the data clearly indicate that infected Gn pigs exhibited pronounced systemic innate and to a lesser extent, pro-inflammatory cytokine responses to acute PDCoV infection.

unpublished). In particular, 3- to 4-fold increases in the pro-inflammatory cytokines observed in the PDCoV-infected Gn pigs 1 and 2 coincided with the decreased or loss of appetite following acute PDCoV infection in young suckling piglets (Langhans, 2000). However, the potentially beneficial or detrimental effects or roles of these innate and pro-inflammatory cytokines in PDCoV-infected piglets need to be studied further.

5. Conclusion

In addition to LLC-PK or ST cells of swine origin which have been used for the isolation and propagation of PDCoV, our present study revealed that IPEC-J2 cells are also susceptible to infection with PDCoV. However, unlike LLC-PK or ST cells, PDCoV may not induce apoptosis in the infected IPEC-J2 cells, but possibly necrosis, similar to necrotic cell death in infected intestinal enterocytes *in vivo*. Based on these observations, a study of the mechanisms related to cell death caused by PDCoV in IPEC-J2 cells may be applicable to a more comprehensive understanding of cell death of infected enterocytes that occurs *in vivo*. Our findings also indicate the potential usefulness of IPEC-J2 cells: i) to better mimic *in vivo* conditions of PDCoV infection in the small intestine of pigs; ii) to study possible differences in the interactions of enterocytes with distinct swine enteric coronaviruses, PDCoV, PEDV, or TGEV; and iii) to investigate the virus-virus interactions between the viruses when co-infected in IPEC-J2 cells. Additionally, our study demonstrated that the IPEC-J2 cell culture-passaged PDCoV (OH-FD22-P8-I-P4) was enteropathogenic in Gn pigs, and that induction of systemic innate and pro-inflammatory cytokine responses occurred in Gn pigs during the acute PDCoV infection.

Conflict of interest statement

None of the authors of this paper have a financial or personal relationship with other people or organizations that could inappropriately influence or bias the content of the paper.

Acknowledgements

We thank Xiaohong Wang and Marcia Lee for technical assistance. Salaries and research support were provided by state and federal funds appropriated to the Ohio Agricultural Research and Development Center, The Ohio State University.

Appendix A. Supplementary data

Supplementary material related to this article can be found, in the online version, at doi:https://doi.org/10.1016/j.vetmic.2018.05.019.

References

Annamalai, T., Saif, L.J., Lu, Z., Jung, K., 2015. Age-dependent variation in innate immune responses to porcine epidemic diarrhea virus infection in suckling versus weaned pigs. Vet. Immunol. Immunopathol. 168, 193–202.
Brosnahan, A.J., Brown, D.R., 2012. Porcine IPEC-J2 intestinal epithelial cells in microbiological investigations. Vet. Microbiol. 156, 229–237.
Chattha, K.S., Vlasova, A.N., Kandasamy, S., Rajashekara, G., Saif, L.J., 2013. Divergent immunomodulating effects of probiotics on T cell responses to oral attenuated human rotavirus vaccine and virulent human rotavirus infection in a neonatal gnotobiotic piglet disease model. J. Immunol. 191, 2446–2456.
Chen, Q., Gauger, P., Stafne, M., Thomas, J., Arruda, P., Burrough, E., Madson, D., Brodie, J., Magstadt, D., Derscheid, R., Welch, M., Zhang, J., 2015. Pathogenicity and pathogenesis of a United States porcine deltacoronavirus cell culture isolate in 5-day-old neonatal piglets. Virology 482, 51–59.
Gimeno Brias, S., Stack, G., Stacey, M.A., Redwood, A.J., Humphreys, I.R., 2016. The role of IL-22 in viral infections: paradigms and paradoxes. Front. Immunol. 7, 211.
Grunnet, L.G., Aikin, R., Tonnesen, M.F., Paraskevas, S., Blaabjerg, L., Storling, J., Rosenberg, L., Billestrup, N., Maysinger, D., Mandrup-Poulsen, T., 2009. Proinflammatory cytokines activate the intrinsic apoptotic pathway in beta-cells. Diabetes 58, 1807–1815.
Guo, X., Hu, H., Chen, F., Li, Z., Ye, S., Cheng, S., Zhang, M., He, Q., 2016. iTRAQ-based comparative proteomic analysis of vero cells infected with virulent and CV777 vaccine strain-like strains of porcine epidemic diarrhea virus. J. Proteom. 130, 65–75.
Hofmann, M., Wyler, R., 1988. Propagation of the virus of porcine epidemic diarrhea in cell culture. J. Clin. Microbiol. 26, 2235–2239.
Hu, H., Jung, K., Vlasova, A.N., Chepngeno, J., Lu, Z., Wang, Q., Saif, L.J., 2015. Isolation and characterization of porcine deltacoronavirus from pigs with diarrhea in the United States. J. Clin. Microbiol. 53, 1537–1548.
Hu, H., Jung, K., Vlasova, A.N., Saif, L.J., 2016. Experimental infection of gnotobiotic pigs with the cell-culture-adapted porcine deltacoronavirus strain OH-FD22. Arch. Virol. 161, 3421–3434.
Jung, K., Saif, L.J., 2017. Goblet cell depletion in small intestinal villous and crypt epithelium of conventional nursing and weaned pigs infected with porcine epidemic diarrhea virus. Res. Vet. Sci. 110, 12–15.
Jung, K., Wang, Q., Scheuer, K.A., Lu, Z., Zhang, Y., Saif, L.J., 2014. Pathology of US porcine epidemic diarrhea virus strain PC21A in gnotobiotic pigs. Emerg. Infect. Dis. 20, 662–665.
Jung, K., Annamalai, T., Lu, Z., Saif, L.J., 2015a. Comparative pathogenesis of US porcine epidemic diarrhea virus (PEDV) strain PC21A in conventional 9-day-old nursing piglets vs. 26-day-old weaned pigs. Vet. Microbiol. 178, 31–40.
Jung, K., Hu, H., Eyerly, B., Lu, Z., Chepngeno, J., Saif, L.J., 2015b. Pathogenicity of 2 porcine deltacoronavirus strains in gnotobiotic pigs. Emerg. Infect. Dis. 21, 650–654.
Jung, K., Hu, H., Saif, L.J., 2016. Porcine deltacoronavirus induces apoptosis in swine testicular and LLC porcine kidney cell lines in vitro but not in infected intestinal enterocytes in vivo. Vet. Microbiol. 182, 57–63.
Langhans, W., 2000. Anorexia of infection: current prospects. Nutrition 16, 996–1005.
Lau, S.K., Woo, P.C., Yip, C.C., Fan, R.Y., Huang, Y., Wang, M., Guo, R., Lam, C.S., Tsang, A.K., Lai, K.K., Chan, K.H., Che, X.Y., Zheng, B.J., Yuen, K.Y., 2012. Isolation and

characterization of a novel Betacoronavirus subgroup a coronavirus, rabbit coronavirus HKU14, from domestic rabbits. J. Virol. 86, 5481–5496.
Li, W., Hulswit, R.J.G., Kenney, S.P., Widjaja, I., Jung, K., Alhamo, M.A., van Dieren, B., van Kuppeveld, F.J.M., Saif, L.J., Bosch, B.J., 2018. Broad receptor engagement of an emerging global coronavirus may potentiate its diverse cross-species transmissibility. Proc. Natl. Acad. Sci. U. S. A. http://dx.doi.org/10.1073/pnas.1802879115.
Lin, H., Li, B., Chen, L., Ma, Z., He, K., Fan, H., 2017. Differential protein analysis of IPEC-J2 cells infected with porcine epidemic diarrhea virus pandemic and classical strains elucidates the pathogenesis of infection. J. Proteome Res. 16, 2113–2120.
Oka, T., Saif, L.J., Marthaler, D., Esseili, M.A., Meulia, T., Lin, C.M., Vlasova, A.N., Jung, K., Zhang, Y., Wang, Q., 2014. Cell culture isolation and sequence analysis of genetically diverse US porcine epidemic diarrhea virus strains including a novel strain with a large deletion in the spike gene. Vet. Microbiol. 173, 258–269.
Salguero, F.J., Sanchez-Cordon, P.J., Nunez, A., Fernandez de Marco, M., Gomez-Villamandos, J.C., 2005. Proinflammatory cytokines induce lymphocyte apoptosis in acute African swine fever infection. J. Comp. Pathol. 132, 289–302.
Shi, W., Jia, S., Zhao, H., Yin, J., Wang, X., Yu, M., Ma, S., Wu, Y., Chen, Y., Fan, W., Xu, Y., Li, Y., 2017. Novel approach for isolation and identification of porcine epidemic diarrhea virus (PEDV) strain NJ using porcine intestinal epithelial cells. Viruses 9. http://dx.doi.org/10.3390/v9010019.
Azevedo, M.S., Yuan, L., Pouly, S., Gonzales, A.M., Jeong, K.I., Nguyen, T.V., Saif, L.J., 2006. Cytokine responses in gnotobiotic pigs after infection with virulent or attenuated human rotavirus. J. Virol. 80, 372–382.
Vergauwen, H., 2015. The IPEC-J2 cell line. In: Verhoeckx, K.e.a. (Ed.), The Impact of Food Bio-Actives on Gut Health, pp. 125–134.
Wang, B., Liu, Y., Ji, C.M., Yang, Y.L., Liang, Q.Z., Zhao, P., Xu, L.D., Lei, X.M., Luo, W.T., Qin, P., Zhou, J., Huang, Y.W., 2018. Porcine deltacoronavirus engages the transmissible gastroenteritis virus functional receptor porcine aminopeptidase N for infectious cellular entry. J. Virol. http://dx.doi.org/10.1128/JVI.00318-18.
Xia, L., Dai, L., Yu, Q., Yang, Q., 2017. Persistent TGEV infection enhances ETEC K88 adhesion by promoting epithelial-mesenchymal transition in intestinal epithelial cells. J. Virol. 91 (21), e01256-17. http://dx.doi.org/10.1128/JVI.01256-17.
Zhang, Q., Yoo, D., 2016. Immune evasion of porcine enteric coronaviruses and viral modulation of antiviral innate signaling. Virus Res. 226, 128–141.
Zhang, Q., Ke, H., Blikslager, A., Fujita, T., Yoo, D., 2018. Type III interferon restriction by porcine epidemic diarrhea virus and the role of viral protein nsp1 in IRF1 signaling. J. Virol. 92, e01677-17. http://dx.doi.org/10.1128/JVI.01677-17.
Zhao, S., Gao, J., Zhu, L., Yang, Q., 2014. Transmissible gastroenteritis virus and porcine epidemic diarrhoea virus infection induces dramatic changes in the tight junctions and microfilaments of polarized IPEC-J2 cells. Virus Res. 192, 34–45.
Zhu, X., Liu, S., Wang, X., Luo, Z., Shi, Y., Wang, D., Peng, G., Chen, H., Fang, L., Xiao, S., 2018. Contribution of porcine aminopeptidase n to porcine deltacoronavirus infection. Emerg. Microbes Infect. 7, 65.